01 Dec 2011

The Role of Eddies inside Pores in the Transition from Darcy to Forchheimer Flows

Kuldeep Chaudhary

M. Bayani Cardenas

Wen Deng
Missouri University of Science and Technology, wendeng@mst.edu

Philip C. Bennett

Recommended Citation

K. Chaudhary et al., "The Role of Eddies inside Pores in the Transition from Darcy to Forchheimer Flows," *Geophysical Research Letters*, vol. 38, no. 24, American Geophysical Union (AGU), Dec 2011.
The definitive version is available at https://doi.org/10.1029/2011GL050214

The role of eddies inside pores in the transition from Darcy to Forchheimer flows

Kuldeep Chaudhary,[1] M. Bayani Cardenas,[1] Wen Deng,[1] and Philip C. Bennett[1]

Received 31 October 2011; accepted 12 November 2011; published 30 December 2011.

[1] We studied the role of intra-pore eddies, from viscous to inertial flows, in modifying continuum-scale flow inside pores. Flow regimes spanning Reynolds Number $Re \sim 0$ to 1350 are divided into three zones – one zone follows Darcy flow, and the other two zones describe non-Darcy or Forchheimer flow. During viscous flows, i.e., $Re < 1$, stationary eddies occupy about 1/5 of the pore volume. Eddies grow when $Re > 1$, and their growth leads to the deviation from Darcy's law and the emergence of Forchheimer flow manifested as a characteristic reduction in the apparent hydraulic conductivity K_a. The reduction in K_a is due to the narrowing of the flow channel which is a consequence of the growth in eddies. The two zones of Forchheimer flow correspond to the changes in rate of reduction in K_a, which in turn are due to the changes in eddy growth rate. Since the characteristics of Forchheimer flow are specific to pore geometry, our results partly explain why a variety of Forchheimer models are expected and needed for different porous media.
Citation: Chaudhary, K., M. B. Cardenas, W. Deng, and P. C. Bennett (2011), The role of eddies inside pores in the transition from Darcy to Forchheimer flows, *Geophys. Res. Lett.*, *38*, L24405, doi:10.1029/2011GL050214.

1. Introduction

[2] Flow through porous media is fundamental to many geophysical processes and problems. In 1856, *Henry Darcy* conducted filtration experiments with sediment columns and established a linear relationship between the specific flux, q [m/s] and the hydraulic head gradient, i [−]. This relationship was later derived from first principles and was termed as Darcy's law:

$$q = -Ki \tag{1}$$

where K [m/s] is the hydraulic conductivity, which is the slope of the $q(i)$ relationship. Hydraulic head gradient, $i = dh/dz$; where head, $h = P/\rho g$ [m], P [Pa] is pressure, and z [m] is a one dimensional coordinate. Darcy's law presumes Stokes flow, i.e., Reynolds Number (Re) of ∼0. However, it has been extensively used in geophysical and engineering applications for Re of up to 1. As early as 1863, another French engineer, Jules Dupuit [*Dupuit*, 1863] noted that the linear relationship proposed by Darcy does not hold for higher flow rates. Subsequently, *Forchheimer* [1901] presented data which showed the breakdown of Darcy's law at high flow rates, and thereafter presented an empirical relationship for one dimensional flow which included a squared velocity term:

$$-i = aq + b\ q^2 \tag{2}$$

where a and b are coefficients of the polynomial fit, and from (2) and (1), $1/K_a = a + b\ q$, where K_a is apparent hydraulic conductivity. By the 1960s, several authors presented equations similar in concept to (2) and provided theoretical derivations employing averaging or homogenization of the Navier–Stokes equations. A detailed summary of references from this era can be found in work by *Scheidegger* [1960] and *Bear* [1972]. It was during this period that the breakdown of Darcy's law, which occurs in the laminar flow regime and at high Re, was attributed to inertial forces which dominate over viscous forces as flow rate increases [*Bear*, 1972]. In addition, the cause of deviation at high Re was considered to be due to the separation of flow in pores where flow diverged [*Bear*, 1972; *Irmay*, 1958].

[3] Since not one equation can accurately describe the non-linear flow at high Re, the pursuit of a single constitutive relationship for non-Darcy flow has continued to date. Theoretical studies [*Chen et al.*, 2001; *Hassanizadeh and Gray*, 1987; *Skjetne and Auriault*, 1999a, 1999b] have been complimented by pore-scale numerical simulations [*Fourar et al.*, 2004; *Hlushkou and Tallarek*, 2006; *Panfilov and Fourar*, 2006] and experimental studies [*Chauveteau and Thirriot*, 1967; *Johns et al.*, 2000]. Additional studies can be found in work by *Chen et al.* [2001], *Hlushkou and Tallarek* [2006], *Balhoff and Wheeler* [2009], and *McClure et al.* [2010].

[4] Despite extensive previous work, our understanding about the physical reasons for non-Darcy flow is incomplete [*Hlushkou and Tallarek*, 2006]. Briefly summarizing from the recent literature, the commonly cited cause for the deviation from Darcy's law is 'effects of inertia' which is manifested by the following: formation of a viscous boundary layer [*Whitaker*, 1996], the interstitial drag force [*Hassanizadeh and Gray*, 1987; *Ma and Ruth*, 1993], singularity of streamline patterns [*Panfilov et al.*, 2003], separation of flow [*Skjetne and Auriault*, 1999b], and deformation of streamline patterns and formation of eddies [*Fourar et al.*, 2004; *McClure et al.*, 2010; *Panfilov and Fourar*, 2006]. While these reasons either have a theoretical origin or are qualitative descriptions of the modified flow field, they do not explain how the formation of eddies or singularities in the flow field contribute to the non-linear flow characteristics. The non-linear or non-Darcy flow is a manifestation of a characteristic decrease in hydraulic conductivity (K) at increasing Re flows, and the cause for this characteristic decrease in K remains to be explored in depth.

[5] In this paper, we specifically address questions such as: *How and why do eddies lead to deviation from Darcy's law at increasing Re flows? How does this deviation result*

[1]Geological Sciences, University of Texas at Austin, Austin, Texas, USA.

0094-8276/11/2011GL050214

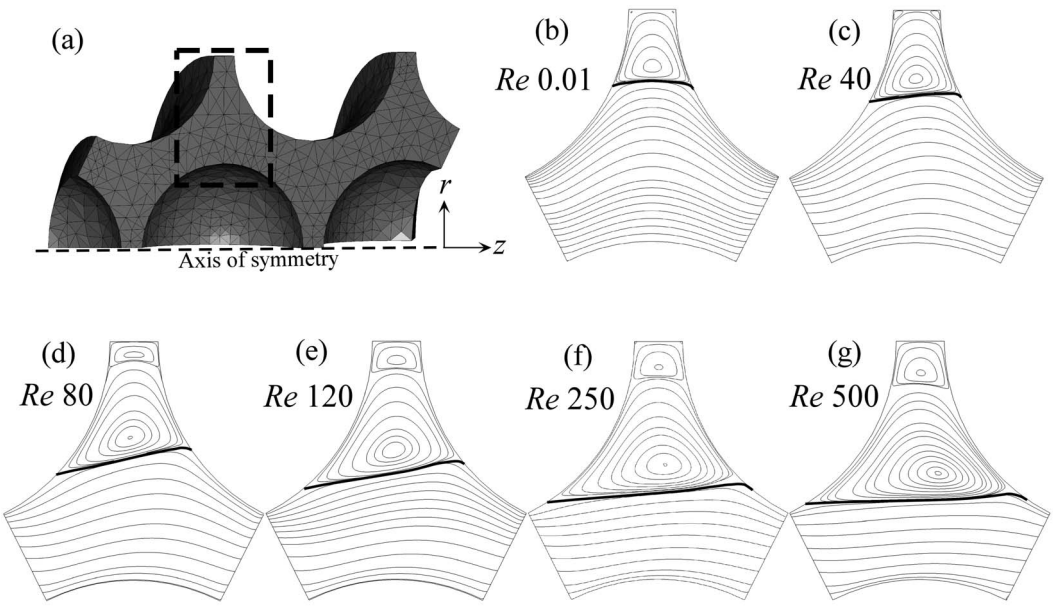

Figure 1. (a) 3-D rendition of 1/4th of the axis symmetric pores formed due staggered pattern of spheres. (b) Flow field shows a pair of corner eddies and a larger stationary eddy in the Darcy flow regime. (c) to (g) growth in eddies as flow rates increases from *Re* 0.01 to *Re* 500 to occupy a large part of the advective pore volume (n_e). Bold black lines point at the separation between zones occupied by eddies and n_e. Thin black lines are streamlines.

in a decrease in hydraulic conductivity? How does the dynamic growth behavior of eddies influence Forchheimer flow characteristics? We address these related questions by examining the micro-scale flow fields obtained via pore-scale computational fluid dynamics (CFD) simulations on an axis-symmetric converging–diverging pore, which represents a part of pores formed due to the staggered pattern of spherical grains (Figure 1a). A series of steady-state flow fields are obtained by imposing stepwise increase in head gradient. The resultant flow behavior is distinguished into three zones based on functional forms of $q(i)$. The first zone shows where Darcy's law is valid and where the inertial forces are presumed negligible. The next two zones show non-Darcy or Forchheimer flow and represent the dominance of inertial effects. Our results show how an increase in inertia at increasing *Re* flows leads to the deviation from Darcy's law and a decrease in hydraulic conductivity as the flow becomes non-linear. Later, we analyze Forchheimer flow characteristics and explain the origin of its two zones.

2. Methods: Numerical Simulation Scheme and Experimental Pore Design

[6] We conducted the CFD simulations in an axis-symmetric framework to represent the process in three dimensions while modeling it in two dimensions (Figure 1a). The axis of symmetry is at the center of spherical grains, which are arranged in a staggered pattern. We chose a staggered pattern to represent the tortuous flow paths inherent in geologic porous media. Therefore, the flow domain we investigate is the network of flow channels wrapped around spherical grains (Figure 1a). The spherical grains have a radius of 10^{-3} m, and pore-throats are 5×10^{-4} m in the direction of flow (inlet and outlet) and 2.5×10^{-4} m perpendicular to the flow direction.

[7] Steady incompressible flow is governed by the Navier-Stokes and the continuity equations:

$$\nabla P = \mu \nabla^2 \boldsymbol{u} - \rho(\boldsymbol{u} \cdot \nabla)\boldsymbol{u} \tag{3}$$

$$\nabla \cdot \boldsymbol{u} = 0 \tag{4}$$

where ρ is fluid density, $\boldsymbol{u} = [u, v, w]$ is the velocity vector, μ is dynamic viscosity, and P is total pressure. Standard fluid properties for water are used: $\rho = 1000$ kg/m^3, and $\mu = 0.001$ Pa-s.

[8] Numerical solutions are obtained via the finite-element method implemented with COMSOL Multiphysics. Lagrange-triangular elements are used to discretize the domain. The governing equations are cast and solved in cylindrical coordinates (r, z).

[9] The center of spheres is an axis of symmetry (Figure 1a). The grain surfaces and the pore throat perpendicular to the z-axis follow no-slip or wall boundary conditions. Inlet and outlet boundaries, which are pore throats perpendicular to the r-axis, are periodic boundaries with a pressure drop. Therefore, the solutions represent a single pore from an infinite sequence of pores draped around spheres in a staggered pattern (Figure 1a). The pressure drop is systematically increased from 10^{-3} Pa to 250 Pa across the pore to obtain flow regimes of *Re* from ~0 to 1350.

3. Results and Discussion

[10] In ensuing discussion, the Reynolds Number *Re* [−] is given by:

$$Re = \frac{\rho\ \bar{U} d_0}{\mu} \tag{5}$$

where $\bar{U}$ is the average velocity at the inlet and d_0 is the diameter of the spherical grain.

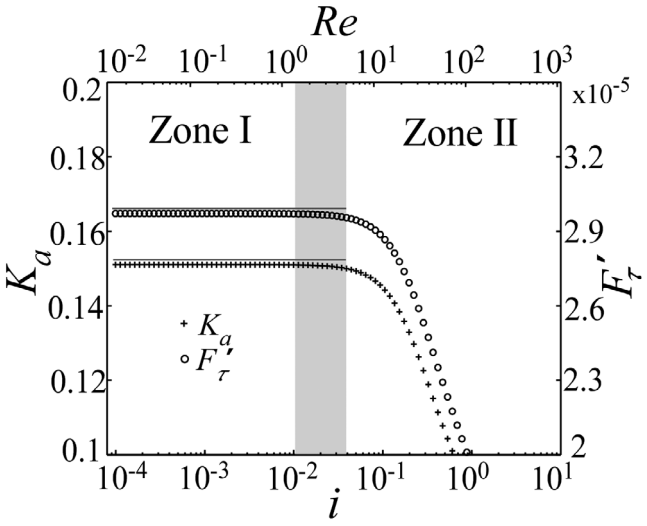

Figure 2. The deviation from Darcy's law shown by the non-linearity in apparent hydraulic conductivity K_a [m/s] and rate of change in friction drag [N] at increasing hydraulic gradient i [−]. Zone I shows where Darcy's law is valid and Zone II marks the emergence of the Forchheimer flow regime.

3.1. Persistent Eddies at $Re \ll 1$

[11] At *Re* 0.014, which is equivalent to a dimensionless head gradient i of 9×10^{-5}, a pair of corner eddies and a larger stationary eddy are observed in the pore body (Figure 1b). *Cardenas* [2008] has similarly shown three dimensional eddies inside a pore at i of 1.02×10^{-6} and also in simulations solving the Stokes equations [*Cardenas et al.*, 2009]. Eddies existing at *Re* 0.84 has also been observed in experiments using MRI [*Johns et al.*, 2000]. At these flow conditions on the order of 10^{-5} m/s, Darcy's law holds (Stokes flow regime), yet eddies exist mainly due to the geometry of the diverging–converging pore. This is similar to early descriptions by *Moffatt* [1964] that eddies form around sharp corners even in the Stokes flow regime. These eddies are often called *Moffatt eddies*, *Stokes eddies*, or *viscous eddies*. It is thus important to note that in extremely slow flow conditions when viscous forces dominate over inertial forces, eddies are present, which is counter to the widely-held notion that eddies form when inertial forces begin to dominate, i.e., at $Re \gg 1$ [*Bear*, 1972; *Chauveteau and Thirriot*, 1967; *Fourar et al.*, 2004; *McClure et al.*, 2010; *Panfilov et al.*, 2003].

[12] At *Re* 0.01, stationary eddies occupy about 18% of the total pore volume, and at these extremely slow flows, their size is entirely dependent on the pore geometry. If we consider the geometry of real pores in geologic porous media, they have sharp corners especially due to secondary diagenetic alterations, which indicate that geologic porous media likely have eddies at all flow conditions.

3.2. Deviation From Darcy's Law

[13] The cause for the deviation from Darcy's law has been attributed to the generation of eddies within the microscale flow field [*Fourar et al.*, 2004; *McClure et al.*, 2010; *Panfilov and Fourar*, 2006; *Panfilov et al.*, 2003]. If eddies were to form at some threshold *Re* where inertial forces begin to dominate over viscous forces, we can expect an abrupt change in the flow or stress field that might lead to a potentially abrupt variation in the $q(i)$ relationship. On the contrary, we observed that the deviation from Darcy's law with increasing q is very gradual (Figure 2).

[14] The gradual deviation from Darcy's law is due to the gradual growth of pre-existing eddies (discussed in section 3.1) with an increase in i (Figures 1b and 1c). By continuously increasing the flow rate, the angular velocity of an eddy increases, i.e., its inertial/centrifugal force increases. And, as the inertial force of an eddy surpasses the surrounding pressure force, the eddy begins to grow. We quantify eddy growth by quantifying the viscous force or friction drag F_τ on the pore boundaries (Figure 1a). In the laminar flow regime, F_τ is expected to increase linearly with an increase in i. However, the net rate of increase in F_τ will likely decrease as an eddy begins to grow, because as an eddy grows, a larger area of the pore boundary is subjected to counter flow which contributes negative friction drag. The z-component of the friction drag in the cylindrical coordinates is:

$$\boldsymbol{F}_{\tau,z} = \eta\left[\left(\frac{\partial u}{\partial z} + \frac{\partial v}{\partial r}\right)\cdot \boldsymbol{n_r} + 2\left(\frac{\partial v}{\partial z}\right)\cdot \boldsymbol{n_z}\right] \tag{6}$$

where, η is the dynamic viscosity, u and v are velocities in r-direction and z-direction, respectively, and $\boldsymbol{n_r}$ and $\boldsymbol{n_z}$ are unit vectors in r- and z-directions, respectively. In an axis symmetric tube, the net friction drag per unit surface area F_τ is calculated by integrating the z-component of the friction drag over the surface of pore body as:

$$F_\tau = \frac{\int \boldsymbol{F}_{\tau,z}\cdot \boldsymbol{t}\, dA}{\int dA} \tag{7}$$

where $\boldsymbol{t}$ is the unit vector tangent to pore boundaries. Since the integration of the friction drag's r-component over the surface of an axis symmetric tube yields zero, it is not included here. The rate of change in F_τ with increasing i is:

$$F'_\tau = \frac{\partial F_\tau}{\partial i} \tag{8}$$

Corresponding to the functional form $q(i)$, we define an apparent hydraulic conductivity (K_a) following (1).

[15] At $Re < 1$, both K_a and F_τ' are insensitive to increasing i (Figure 2) clearly delineating a zone where Darcy's law is valid (Zone I in Figure 2). Even though, eddies are present in Zone I flow regime, F'_τ does not change with i, indicating that neither do eddies grow in Zone I flow regime, nor do they affect the $q(i)$ relationship (Figures 1b and 2). In Zone I flow regime, K_a is the true hydraulic conductivity K in (1).

[16] At flows of $Re > 1$, both K_a and F'_τ begin to decrease congruently marking the deviation from Darcy's law (Zone II in Figure 2). Since K_a decreases simultaneously with a decrease in F'_τ, and since the decrease in F'_τ is a consequence of an increase in size of eddies, the deviation from Darcy's law is a result of growth in eddies.

[17] The usage and definition of *Re* for porous media vary depending on the choice of length scale, i.e., d_o in (5). If we use pore throat as d_o, the deviation from Darcy's law occurs at *Re* 0.3. But if we use grain diameter as d_o, the *Re* at which the deviation occurs becomes 1.5, i.e., *Re* used here

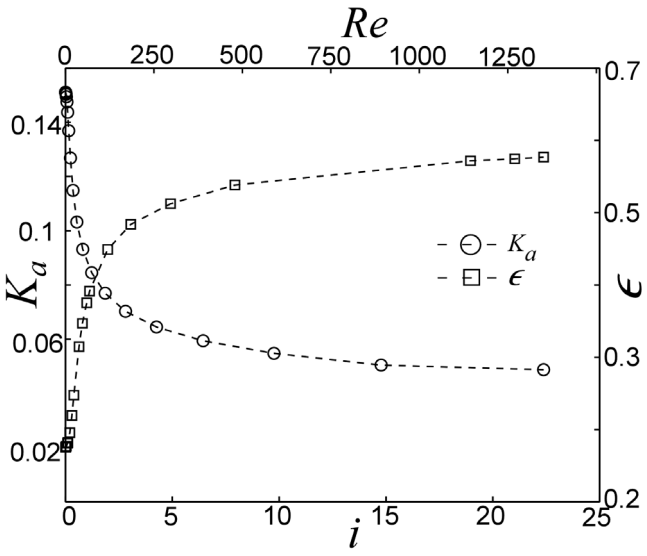

Figure 3. Ratio of growth in eddies ϵ [−] is directly related to a decrease in the apparent hydraulic conductivity K_a [m/s] as the flow rate Re [−] or i [−] increases.

(Figures 1–4) are ∼5× of Re calculated using pore throats. The former description points that the deviation occurs when inertial forces are not dominant ($Re < 1$), but the latter description indicate the breakdown between $1 < Re > 10$, which is consistent with *Bear* [1972].

3.3. The Cause for Decrease in the Apparent Hydraulic Conductivity K_a

[18] Growth in eddies at increasing Re flows is well documented in experiments [*Chauveteau and Thirriot*, 1967] and numerical studies [*Fourar et al.*, 2004; *Skjetne and Auriault*, 1999b], but how their growth contributes to and affects non-Darcy flow is not clear. We show that the decrease or reduction in K_a, which is the main indicator for non-Darcy flow, is due to the shrinking of advective pore volume (n_e), i.e., the narrowing of the flow channel associated with the growing eddies. The n_e is the contiguous zone covered by the bulk flow. We map and separate the eddy region from the bulk flow (n_e) using streamlines (Figure 1). The ratio of n_e to total pore volume is denoted by α, and 1-α, which is the ratio of eddies to total pore volume, is denoted by 'ϵ'.

[19] The ratio of eddies to total volume ϵ is inversely related to K_a, or, conversely, the ratio of flow channel to total volume α is directly related to K_a (Figure 3). Both α and K_a sharply decrease with increasing i until $Re \sim 450$ and begin to behave asymptotically at $Re > 450$ (Figure 3). The sharp decrease in α at $Re < 450$ is due to a fast initial growth in eddies, whereas the asymptote in α at $Re > 450$ is due to the slowing of growth in eddies. The growth in eddies slows down because, once they have grown to occupy a large part of the pore, their growth becomes limited by pore boundaries and increased pressure at the eddy-bulk flow interface, which is due to the narrowing of flow channel (Figures 1f and 1g). The decrease in K_a with a decrease in n_e or α could be qualitatively explained by using Hagen-Poiseuille's law, in which the 'hydraulic conductivity' of an idealized cylindrical pore (a tube) is nonlinearly related to pore radius $-K \sim R^2$. However, given the geometry of the pore we considered is far from a uniform tube, a variation from $K_a \sim R^2$ sensitivity is expected.

3.4. Forchheimer Flow Characteristics

[20] Whether Forchheimer flow corresponds to when flow rate is dependent on the pressure gradient via a quadratic equation (i.e., (2)), a cubic equation, or a power function, has been a subject of extended and intense debate [*Balhoff and Wheeler*, 2009; *Chen et al.*, 2001; *Cheng et al.*, 2008; *Panfilov and Fourar*, 2006; *Skjetne and Auriault*, 1999a]. While various theoretical explanations justify each of these relationships, several also point out their failure under different flow scenarios. For example, the quadratic law fails at low Re flows [*Balhoff and Wheeler*, 2009]. The physical explanation of why it fails at low Re or why it needs to be described by a cubic equation [*Mei and Auriault*, 1991], described by a 5th order equation [*Balhoff and Wheeler*, 2009], or if it needs an exponential correction [*Panfilov and Fourar*, 2006], continues to be unclear.

[21] We show that the characteristics of Forchheimer flow, which can be separated into two zones, are due to the dynamic growth behavior of eddies in pores. A close examination of the $i(q)$ relationship for non-Darcy flow indicates that in Zone II this relationship follows a power law (Figure 4a) which transitions to another power law in Zone III such that the exponent in the power function for $i(q)$ relationship increases from 1.05 to 1.24 at increasing Re flows (Figure 4a). We further study this distinct flow behavior in Zone II and Zone III by analyzing how K_a and ϵ change in relation to i, i.e., by analyzing the derivatives K_a' and ϵ' following (8). As i increases in Zone II, the absolute value of K_a' increases congruently with an increase in absolute value of eddy growth rate, i.e., $|\epsilon'|$ until they reach a maximum at $Re \sim 20$ with a phase lag of $Re \sim 10$ between $|\epsilon'|$ and K_a' (Figures 4c and 4d). This maximum marks the transition to Zone III, beyond which both $|K_a'|$ and $|\epsilon'|$ decrease congruently at higher i (Figures 4c and 4d). This direct relationship between $|K_a'|$ and $|\epsilon'|$ shows that the characteristics of Forchheimer flow are due to the growth behavior of eddies. In Zone II, the growth rate of eddies increases, while in Zone III, it decreases mostly because, at first, eddies grow almost unaffected by pore boundaries and increase in pressure in the bulk flow area. But later, as they grow to occupy a larger part of the pore volume, their growth becomes limited both by pore boundaries and a higher increase in pressure at the eddy-bulk flow interface, which is related to the narrowing of the flow channel at high Re flows (Figure 1d).

[22] The dynamics of eddy growth largely depend on pore geometry and systematically influence K_a. Moreover, the span of Zone II across the range of i and the nature of the power law obtained in Zone III are also entirely dependent on the dynamics of eddy growth specific to pore geometry, as a function of i. Therefore, at the macro-scale, a combination of effects related to eddy growth behavior inside many pores should be reflected in porous media's K and its small-scale spatial variation. Given that in real porous media there is a large variance in pore geometry, it is unlikely that non- Darcy or Forchheimer flow can be explicitly described by a single function for all porous media and for all high Re flow conditions. Therefore, it is expected that different functions may be needed for site and medium specific scenarios, even up to,

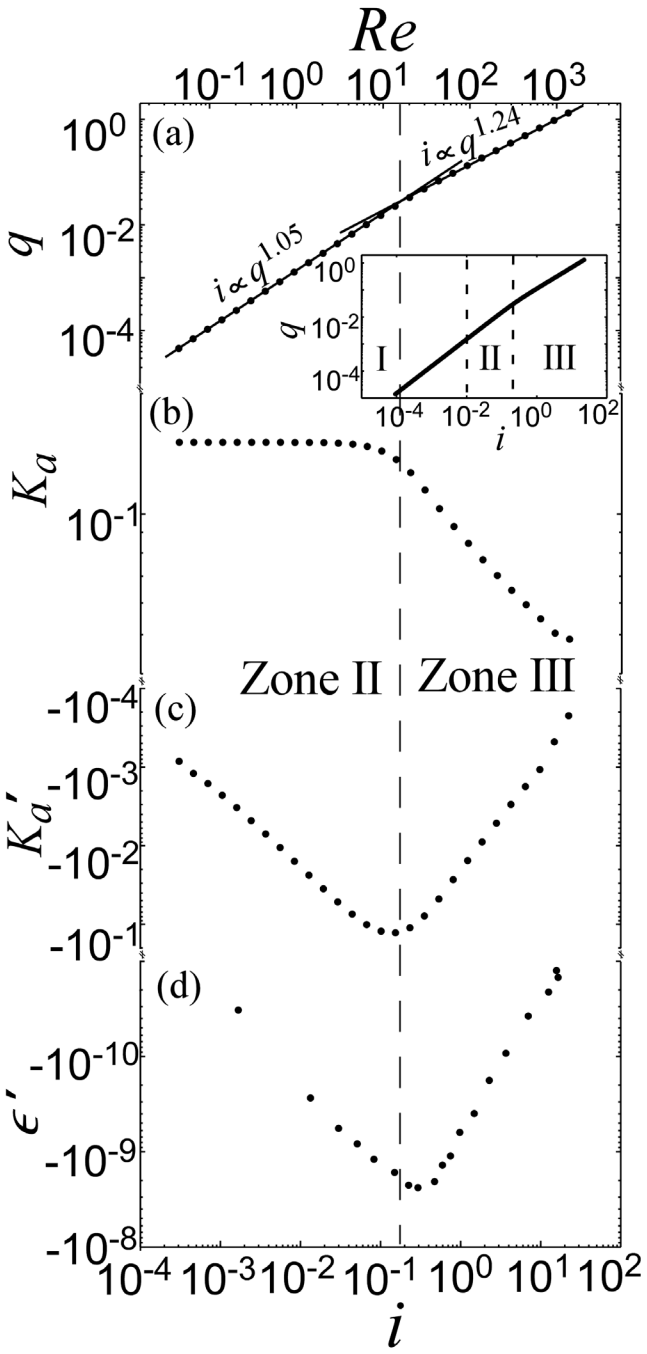

Figure 4. Characteristics of Forchheimer flow in Zone II and Zone III as shown by dependence of: (a) specific flux q [m/s], (b) apparent hydraulic conductivity K_a [m/s], (c) rate of change in apparent hydraulic conductivity K_a' [m/s], and (d) rate of change in eddy growth ϵ' [−], on Re [−] and i [−].

for example, a 5th order polynomial [*Balhoff and Wheeler*, 2009; *Balhoff et al.*, 2010].

4. Summary

[23] a) We have shown that stationary eddies exist in Darcy flow regime, i.e., at $Re \ll 1$, and perhaps exist at all flow conditions in a geologic porous media. The size and frequency of these eddies, however, remains an open question.

[24] b) The deviation from Darcy's law is directly associated with the growth of pre-existing eddies, if any, due to flow rate increase when $Re > 1$.

[25] c) A reduction in the apparent hydraulic conductivity K_a, which is a key indicator for the deviation from Darcy's law, is due to a decrease in advective pore volume (i.e., the narrowing of flow channel) as a consequence of eddy growth at increasing Re flows.

[26] d) The characteristics of non-Darcy or Forchheimer flow are directly related to the dynamic growth behavior of eddies in pores. The two Forchheimer flow zones correspond to a concomitant increase and decrease in the eddy growth rate and the rate of reduction in K_a. At first, the eddy growth rate increases because the growth initially is not much affected by pore boundaries and increase in pressure in the bulk flow area. But later, as eddies grow to occupy a larger part of the pore volume, their growth becomes limited both by pore boundaries and a higher increase in pressure at the eddy-bulk flow interface, which is related to the narrowing of the flow channel.

[27] e) An appropriate functional form for describing macro-scale Forchheimer flow is inherently dependent on combination of effects related to dynamic growth behavior of eddies (dead zones), integrated over all pores in a geological porous medium. Given that there exists a large variation in pore geometries at the macro-scale, different functional forms may be needed to explicitly describe non-Darcy flow for different porous media.

[28] **Acknowledgments.** This material is based upon work supported as part of the Center for Frontiers of Subsurface Energy Security (CFSES) at the University of Texas at Austin, an Energy Frontier Research Center funded by the U.S. Department of Energy, Office of Science, Office of Basic Energy Sciences under award DE-SC0001114. Additional support was provided by the Geology Foundation of the University of Texas.

[29] The Editor thanks the anonymous reviewer.

References

Balhoff, M., and M. F. Wheeler (2009), A predictive pore-scale model for non-Darcy flow in porous media, *SPE J.*, *14*(4), 579–587, doi:10.2118/110838-PA.

Balhoff, M., A. Mikelic, and M. F. Wheeler (2010), Polynomial filtration laws for low Reynolds number flows through porous media, *Transp. Porous Media*, *81*(1), 35–60, doi:10.1007/s11242-009-9388-z.

Bear, J. (1972), *Dynamics of Fluids in Porous Media*, Elsevier, New York.

Cardenas, M. B. (2008), Three-dimensional vortices in single pores and their effects on transport, *Geophys. Res. Lett.*, *35*, L18402, doi:10.1029/2008GL035343.

Cardenas, M. B., D. T. Slottke, R. A. Ketcham, and J. M. Sharp (2009), Effects of inertia and directionality on flow and transport in a rough asymmetric fracture, *J. Geophys. Res.*, *114*, B06204, doi:10.1029/2009JB006336.

Chauveteau, G., and C. Thirriot (1967), Régimes d'écoulement en milieu poreux et limite de la loi de Darcy, *Houille Blanche*, *22*, 1–8.

Chen, Z., S. L. Lyons, and G. Qin (2001), Derivation of the Forchheimer law via homogenization, *Transp. Porous Media*, *44*(2), 325–335, doi:10.1023/A:1010749114251.

Cheng, N. S., Z. Y. Hao, and S. K. Tan (2008), Comparison of quadratic and power law for nonlinear flow through porous media, *Exp. Therm. Fluid Sci.*, *32*(8), 1538–1547, doi:10.1016/j.expthermflusci.2008.04.007.

Dupuit, J. (1863), *Etudes Théoriques et Pratiques sur le Mouvement des Eaux*, Dunod, Paris.

Forchheimer, P. (1901), Wasserbewegung durch Boden, *Z. Ver. Dtsch. Ing.*, *45*, 1736–1741, 1781–1788.

Fourar, M., G. Radilla, R. Lenormand, and C. Moyne (2004), On the non-linear behavior of a laminar single-phase flow through two and three-dimensional porous media, *Adv. Water Resour.*, *27*(6), 669–677, doi:10.1016/j.advwatres.2004.02.021.

Hassanizadeh, S. M., and W. G. Gray (1987), High-velocity flow in porous media, *Transp. Porous Media*, *2*(6), 521–531, doi:10.1007/BF00192152.

Hlushkou, D., and U. Tallarek (2006), Transition from creeping via viscous-inertial to turbulent flow in fixed beds, *J. Chromatogr. A*, *1126*(1–2), 70–85, doi:10.1016/j.chroma.2006.06.011.

Irmay, S. (1958), On the theoretical derivation of Darcy and Forchheimer formulas, *J. Geophys. Res.*, *39*, 702–707.

Johns, M. L., A. J. Sederman, A. S. Bramley, L. F. Gladden, and P. Alexander (2000), Local transitions in flow phenomena through packed beds identified by MRI, *AIChE J.*, *46*(11), 2151–2161, doi:10.1002/aic.690461108.

Ma, H., and D. W. Ruth (1993), The microscopic analysis of high Forchheimer number flow in porous media, *Transp. Porous Media*, *13*(2), 139–160, doi:10.1007/BF00654407.

McClure, J. E., W. G. Gray, and C. T. Miller (2010), Beyond anisotropy: Examining non-Darcy flow in asymmetric porous media, *Transp. Porous Media*, *84*(2), 535–548, doi:10.1007/s11242-009-9518-7.

Mei, C. C., and J. L. Auriault (1991), The effect of weak inertia on flow through a porous medium, *J. Fluid Mech.*, *222*, 647–663, doi:10.1017/S0022112091001258.

Moffatt, H. (1964), Viscous and resistive eddies near a sharp corner, *J. Fluid Mech.*, *18*, 1–18, doi:10.1017/S0022112064000015.

Panfilov, M., and M. Fourar (2006), Physical splitting of nonlinear effects in high-velocity stable flow through porous media, *Adv. Water Resour.*, *29*(1), 30–41, doi:10.1016/j.advwatres.2005.05.002.

Panfilov, M., C. Oltean, I. Panfilova, and M. Bues (2003), Singular nature of nonlinear macroscale effects in high-rate flow through porous media, *C. R. Mech.*, *331*(1), 41–48, doi:10.1016/S1631-0721(02)00012-8.

Scheidegger, A. E. (1960), *The Physics of Flow Through Porous Media*, Univ. of Toronto Press, Toronto, Ont., Canada.

Skjetne, E., and J. L. Auriault (1999a), New insights on steady, non-linear flow in porous media, *Eur. J. Mech. B*, *18*(1), 131–145, doi:10.1016/S0997-7546(99)80010-7.

Skjetne, E., and J. L. Auriault (1999b), High-velocity laminar and turbulent flow in porous media, *Transp. Porous Media*, *36*(2), 131–147, doi:10.1023/A:1006582211517.

Whitaker, S. (1996), The Forchheimer equation: A theoretical development, *Transp. Porous Media*, *25*(1), 27–61, doi:10.1007/BF00141261.

P. C. Bennett, M. B. Cardenas, K. Chaudhary, and W. Deng, Geological Sciences, University of Texas at Austin, 1 University Station, C9000, Austin, TX 78712, USA. (kuldeepchaudhary@mail.utexas.edu)